

Nucleophile-Induced Intramolecular Dipole 1,5-Transfer and 1,6-Cyclization: Experimental and ab Initio Studies of Formation, Thermolysis, and Molecular and Electronic Structures of 3,6-Diphenyl-1-propanesulfenimido-1,2,4,5-tetrazine

Piotr Kaszynski^{*,†} and Victor G. Young, Jr.[‡]

Contribution from the Organic Materials Research Group, Department of Chemistry, Vanderbilt University, Nashville, Tennessee 37235, and X-ray Crystallographic Laboratory, Department of Chemistry, University of Minnesota, Twin Cities, Minnesota 55455

Received November 1, 1999

Abstract: Reaction of dichlorobenzaldazine (**2**) with sodium azide followed by 1-propanethiol/Et₃N furnished tetrazine ylide **1** as the main product. The structure of this unprecedented ylide was confirmed with single-crystal X-ray analysis [C₁₇H₁₇N₅S, monoclinic *P*2₁/*n* *a* = 6.8294(4) Å, *b* = 13.6781(9) Å, *c* = 17.5898(12) Å, β = 90.666(1)°, *Z* = 4] and favorably compared with the results of ab initio calculations. The mechanisms of formation of the ylide and its thermal decomposition to 2,5-diphenyltetrazine (**5**) were investigated using ab initio methods and correlated with the experimental observations. The results suggest that formation of **1** involves intramolecular cyclization of a nitrile imine and thermolysis of **1** might generate a sulfenylnitrene. The formation of **1** is considered to be the first example of a potentially more general reaction.

Introduction

Intramolecular reactions of 1,3-dipoles provide one of the most versatile ways to construct heterocyclic rings.¹ Among these reactions is the cyclization of conjugated dipoles, which typically yields five-membered, and rarely seven-membered rings.^{2,3} To our knowledge, the formation of six-membered rings by cyclization of conjugated 1,3-dipoles has never been observed, and even if the structure permits 1,6-cyclization, formation of a five-membered ring dominates.⁴ Recently, we discovered that certain conjugated 1,3-dipoles readily close to six-membered rings.

In the process of developing an alternative route to 3,6-diphenyl-1,2,4,5-thiatetrazine,⁵ we found that tetrazine **1** is the sole product of a nucleophilic double substitution on dichloride **2** rather than the expected azide **3** or its valence tautomer, tetrazole **4** (Scheme 1). Here we describe the synthesis, molecular structure, and reactivity of the unprecedented tetrazine ylide **1**. The proposed mechanism for its formation from **2** is supported by ab initio calculations and is generalized. Finally, we report kinetic measurements for thermolysis of ylide **1** and discuss the mechanism and product formation in the context of ab initio calculations.

* Author for correspondence. Organic Materials Research Group, Department of Chemistry, Vanderbilt University, Box 1822 Station B, Nashville, TN 37235. Telephone/fax: (615) 322-3458. E-mail: PIOTR@ctrvax.vanderbilt.edu.

† Vanderbilt University.

‡ University of Minnesota.

(1) *1,3-Dipolar Cycloaddition Chemistry*; Padwa, A., Ed.; Wiley & Sons: New York, 1984.

(2) Taylor, E. C.; Turchi, I. J. *Chem. Rev.* **1979**, *79*, 181–231; Huisgen, R. *Angew. Chem. Int. Ed. Engl.* **1980**, *19*, 947–973.

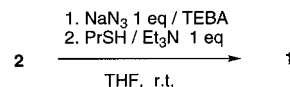
(3) Groundwater, P. W.; Nyerges, M. In *Advances in Heterocyclic Chemistry*; Katritzky, A. R., Ed.; Academic Press: 1999; Vol. 73; pp 97–129.

(4) Hegarty, A. F.; Brady, K.; Mullane, M. *J. Chem. Soc., Perkin Trans. 2* **1980**, 535–540.

(5) Farrar, J. M.; Patel, M. K.; Kaszynski, P.; Young, V. G., Jr. *J. Org. Chem.* **2000**, *65*, 931–940.

Results and Discussion

Synthesis of 1. 3,6-Diphenyl-1-propanesulfenimido-1,2,4,5-tetrazine (**1**) was obtained in a one-pot reaction. Dichloride **2** was reacted with 1 equiv of sodium azide under phase transfer catalysis conditions at room temperature followed by 1 equiv of 1-propanethiol and triethylamine. The major product, tetrazine **1**, was isolated in about 40–50% yield by chromatography as the most polar orange fraction. Neither azide **3** nor tetrazole **4** was identified among the remaining more mobile colorless fractions.



This sequence of reagents, NaN₃ followed by PrSH, was found to be advantageous over the reverse order in which the mercaptan is added first. Reactions of dichloride **2** with sulfur nucleophiles show the tendency for closure of the five-membered thiazazole ring.⁶

¹H NMR analysis of **1** revealed two distinct phenyl rings for which the sets of the ortho hydrogens absorb 0.4 ppm apart (vide infra). The molecule has some spectral characteristics of 3,6-diphenyl-1,2,4,5-tetrazine (**5**). The downfield absorption of a phenyl ring (8.36 ppm) resembles that observed for **5** (8.67 ppm). The resonance at 160.53 ppm, presumably the C⁶ carbon in **1** (Scheme 1), is similar to that ascribed to the C^{3/6} carbon in diphenyltetrazine **5** (164.04 ppm).⁷ The second low-field absorption at 145.78 ppm can be assigned to the C³ carbon in **1** and shows a marked difference in chemical environments for the heterocyclic carbon atoms.

(6) Flowers, W. T.; Robinson, J. F.; Taylor, D. R.; Tipping, A. E. *J. Chem. Soc., Perkin Trans. 1* **1981**, 356–365.

(7) Farkas, L.; Keuler, J.; Wamhoff, H. *Chem. Ber.* **1980**, *113*, 2566–2574.

Scheme 1

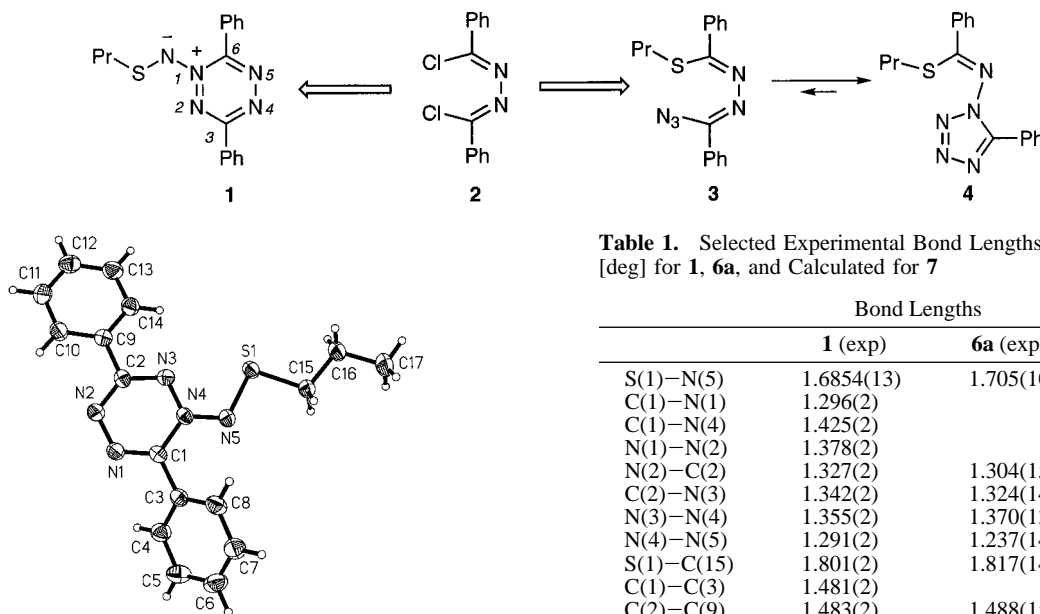


Figure 1. Thermal ellipsoid diagram of tetrazine ylide **1** with the thermal ellipsoids drawn at 50% probability. Hydrogen atoms are given arbitrary radii.

The ^1H chemical shift (3.22 ppm) of the α CH_2 in the propyl group is about 0.5 ppm downfield from a value for a typical sulfide and is consistent with shifts expected for alkylthiodiazenes^{8,9} (e.g.,⁹ 2.85 ppm in $\text{CH}_3\text{S}-\text{N}=\text{N}-\text{Ar}$ vs 2.60 ppm in $\text{CH}_3\text{S}-\text{Ar}$).

Molecular and Crystal Structures for 1. X-ray analysis of a monoclinic crystal of **1** revealed a nearly planar substituted tetrazine ring as shown in Figure 1.¹⁰ Selected bond lengths and angles for **1** are shown in Table 1.

The tetrazine ring in **1** is nearly planar with the largest deviation from the plane by $2.7(2)^\circ$ observed for the $\text{N}(2)\text{C}(2)\text{N}(3)\text{N}(4)$. The sum of the intra-ring angles is $719.95(13)^\circ$, which is indistinguishable from the 720° required for a planar hexagon. The tetrazine ring, however, exhibits a significant in-plane distortion from the geometry observed in 2,6-diphenyl-1,2,4,5-tetrazine¹¹ (**5**) and other phenyl derivatives of 1,2,4,5-tetrazine.^{12,13} The shortest observed C–N bond in **1** is 1.296(2) Å for $\text{C}(1)-\text{N}(1)$ and the longest is 1.425(2) for $\text{C}(1)-\text{N}(4)$, while the C–N distance in the tetrazine derivatives is about 1.34 Å. The short C–N bond is a full double bond (cf. 1.281 Å for $\text{C}=\text{N}$ in oximes),¹⁴ and the long one a single C–N bond (cf. 1.431 Å for C–N in azoarenes).¹⁴ The two N–N distances in **1**, 1.378(2) Å and 1.355(2) Å, are longer than a typical value of about 1.32 Å found in phenyltetrazines,^{11–13} indicative of high single bond character.¹⁴

(8) Fourrey, J.-L.; Henry, G.; Jouin, P. *Nouv. J. Chem.* **1978**, 2, 397–399.

(9) Lerch, U.; Moffatt, J. G. *J. Org. Chem.* **1971**, 36, 3861–3869.

(10) Crystal data for **1**: $\text{C}_{17}\text{H}_{17}\text{N}_5\text{S}$ monoclinic, $P2_1/n$, $a = 6.8294(4)$ Å, $b = 13.6781(9)$ Å, $c = 17.5898(12)$ Å, $\beta = 90.666(1)^\circ$, $V = 1643.0(2)$ Å³, $Z = 4$, $T = 173(2)$ K, $\lambda = 0.71073$ Å, $R(F^2) = 0.0323$ (for 2176 reflections with $I > 2\sigma(I)$), $R(F^2) = 0.0498$ (for all data, 2895 reflections). For details see Supporting Information.

(11) Ahmed, N. A.; Kitaigorodsky, A. I. *Acta Crystallogr.* **1972**, B28, 739–742.

(12) Antipin, M. Y.; Timofeeva, T. V.; Yufit, D. S.; Sauer, J. *Russ. Chem. Bull.* **1995**, 44, 2337–2345.

(13) Breu, J.; Range, K.-J.; Biedermann, N.; Schmid, K.; Sauer, J. *Acta Crystallogr.* **1996**, C52, 936–940.

(14) Allen, F. H.; Kennard, O.; Watson, D. G.; Brammer, L.; Orpen, A. G.; Taylor, R. *J. Chem. Soc., Perkin Trans. 2* **1987**, S1–S19.

Table 1. Selected Experimental Bond Lengths [Å] and Angles [deg] for **1**, **6a**, and Calculated for **7**

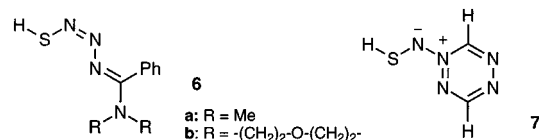
	Bond Lengths		
	1 (exp)	6a (exp) ^b	7 (calcd) ^a
S(1)–N(5)	1.6854(13)	1.705(10)	1.697
C(1)–N(1)	1.296(2)		1.258
C(1)–N(4)	1.425(2)		1.413
N(1)–N(2)	1.378(2)		1.352
N(2)–C(2)	1.327(2)	1.304(15)	1.291
C(2)–N(3)	1.342(2)	1.324(14)	1.337
N(3)–N(4)	1.355(2)	1.370(13)	1.318
N(4)–N(5)	1.291(2)	1.237(14)	1.238
S(1)–C(15)	1.801(2)	1.817(14)	
C(1)–C(3)	1.481(2)		
C(2)–C(9)	1.483(2)	1.488(15)	

	Angles		
	1 (exp)	6a (exp) ^b	7 (calcd) ^a
N(5)–S(1)–C(15)	95.61(7)	93.7(7)	91.6 (NSH)
N(1)–C(1)–N(4)	119.70(14)		121.4
C(1)–N(1)–N(2)	121.67(13)		121.1
C(2)–N(2)–N(1)	115.98(13)		115.3
N(2)–C(2)–N(3)	127.28(14)	118.0(10)	128.8
C(2)–N(3)–N(4)	115.10(13)	114.5(9)	114.3
N(5)–N(4)–N(3)	119.11(12)	115.9(10)	123.1
N(3)–N(4)–C(1)	120.22(13)		119.1
N(4)–N(5)–S(1)	112.10(10)	117.8(9)	115.0

	Angles		
	1 (exp)	6a (exp) ^b	7 (calcd) ^a
N(1)–C(1)–N(4)–N(3)	–0.1(2)		0.0
C(2)–N(3)–N(4)–C(1)	–2.1(2)		0.0
C(1)–N(4)–N(5)–S(1)	179.58(10)		180.0

^a Gas phase calculation (HF/6-31+G*) at the C_s symmetry. ^b Beddoes, R. L.; Mills, O. S. *J. Chem. Res. (M)* **1981**, 5, 1701–1711.

The propanesulfenimido group adopts an all-trans conformation and is nearly coplanar with the tetrazine ring. The largest deviation is observed for the propyl group, which forms a dihedral angle with the ring of 6° . In comparison with the endocyclic N–N bonds, the exocyclic N–N bond is rather short, and its length of 1.291(2) Å is indicative of a conjugated double bond (cf. 1.255 Å for $\text{N}=\text{N}$ in azoarenes).¹⁴ The $\text{S}(1)-\text{N}(5)$ and $\text{C}(15)-\text{S}(1)$ distances (1.6854(13) Å and 1.801(2) Å, respectively) are typical for the corresponding single bonds. Thus, the fragment $\text{C}_3\text{H}_7-\text{S}(1)-\text{N}(5)-\text{N}(4)-\text{N}(3)$ is more properly described as 1-propylthiotriazene group with the $\text{N}(4)$ lone pair coordinating the electron-deficient carbon atom $\text{C}(1)$. Indeed, molecular dimensions of this fragment in **1** correspond well to the analogous values found in the planar **6a**¹⁵ and **6b**¹⁶ (Table 1).



The solid-state geometry of the heterocyclic ring in **1** is consistent with the results of gas-phase ab initio calculations

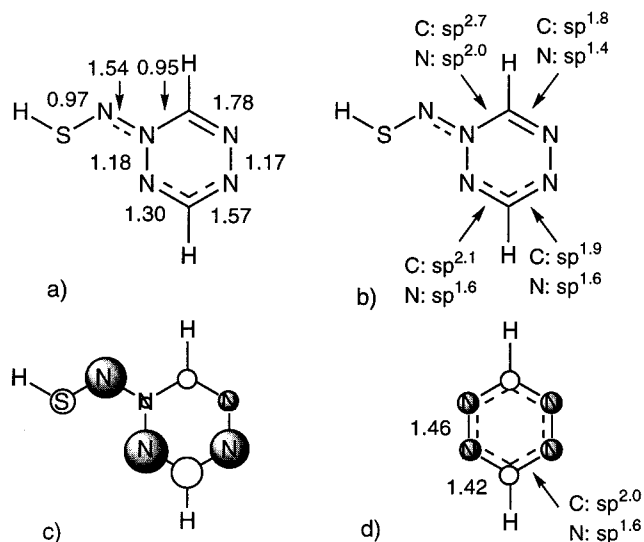


Figure 2. (a) NBO-calculated Wiberg bond order indices, (b) orbital hybridization, and relative atomic charges for (c) the parent ylide **7** and (d) the tetrazine **8**. Full circles represent negative charge density, and dashed lines represent partial double bonds.

for the parent ylide **7** (Table 1). Geometry optimization of **7** shows a planar structure of the ylide (C_s symmetry) with significantly alternating intra-ring bond lengths. The largest differences between the calculated and experimental values are observed for the C(1)–N(1), C(2)–N(2), and N(3)–N(4) bond lengths (about 0.04 Å) and associated angles (about 2°).

The C(3)–C(8) and C(9)–C(14) phenyl rings are planar and are twisted with respect to the tetrazine plane by 38° and 15°, respectively. These relatively large dihedral angles are rather unusual for phenyl derivatives of tetrazine, which are typically coplanar in the solid state.^{11,13} The large dihedral angle formed by the former phenyl ring presumably results from steric interactions between H(8)···N(5) separated only by 2.416 Å. This is less than the value of 2.59 Å typically observed for the nonbonding H···N in organic crystals¹⁷ including phenyltetrazines (2.53 Å).¹² The lack of coplanarity of the two rings disrupts the intermolecular π – π stacking and allows for the other phenyl ring to twist with respect to the tetrazine ring leaving the ortho hydrogen atoms in 2.55 and 2.425 Å distances from the nitrogen atoms.

In the crystal, molecules are parallel within stacks and antiparallel between the stacks. No significant intermolecular close contacts have been observed.

Electronic Structure of 1. The observed bond length alternation in **1** is consistent with the results of NBO¹⁸ analysis of the parent $1A'$ ylide **7** (Figure 2). The Wiberg bond order indices (WBOI) for **7** show that the tetrazine ring has three single bonds, C(1)–N(4) and two N–N bonds (WBOI = 0.95–1.17), a nearly complete double bond, C(1)–N(1) (WBOI = 1.78), and two partial double bonds formed by the C(2) amidinyl carbon (Figure 2a). This is in sharp contrast to results for tetrazine **8** (WBOI \approx 1.45; Figure 2d) and indicates that the heterocyclic ring in **1** has non-aromatic character.

The calculated charge distribution in **7** (Figure 2c) is consistent with the ylide structure. The N(4) nitrogen atom has

(15) Beddoes, R. L.; Mills, O. S. *J. Chem. Res. (M)* **1981**, 5, 1701–1711.

(16) L'abbé, G.; Willcox, A. *Bull. Soc. Chim. Belg.* **1979**, 88, 107–108.

(17) Rowland, R. S.; Taylor, R. *J. Phys. Chem.* **1996**, 100, 7384–7391.

(18) Glendening, E. D.; Reed, A. E.; Carpenter, J. E.; Weinhold, F. *NBO, Version 3.1*.

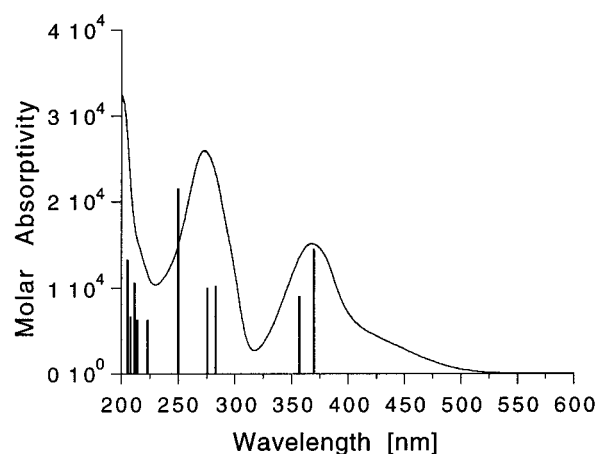


Figure 3. Electronic absorption spectrum for tetrazine ylide **1** recorded in cyclohexane. Vertical lines represent the ZINDO-calculated major transitions scaled by 4.1×10^4 .

a small positive charge which results from the formation of the dative bond between its lone electron pair and C(1) atom. The negative charge is delocalized mainly on the electronegative adjacent nitrogen atoms N(3) and N(5) and the conjugated N(2) atom. This is again in contrast to tetrazine **8** in which the C–N bonds are polarized to a much lower degree than those in **7** (Figure 2d).

The Electronic Absorption Spectrum of 1. The UV spectrum of tetrazine ylide **1** consists of three bands at 368, 274, and about 200 nm, and a broad absorption band tailing to about 510 nm, which is responsible for the orange-yellow color of the compound (Figure 3). This spectrum is markedly different from that of 2,6-diphenyl-1,2,4,5-tetrazine (**5**), which exhibits a weak transition at 544 nm (MeOH) in addition to a strong band at 294 nm.⁷

According to ZINDO calculations for **1**, the long wavelength absorption at 368 nm results from the HOMO–LUMO transition, involving mainly the sulfenimidotetrazine π electron manifold, and HOMO–LUMO+1 transition, which includes the π^* orbital extending over the three rings as shown in Figure 4. The FMOs of **1** are qualitatively identical to those calculated for the parent ylide **7** (see Supporting Information).

The lowest-energy transition for **1** involving the nitrogen lone pairs is calculated to occur at 352 nm. The same absorption for 2,6-diphenyltetrazine (**5**) is found⁷ at 544 nm and calculated at 498 nm.

The strong absorption band at 274 nm is a combination of electronic transitions involving mainly electrons of nitrogen atom lone pairs and the phenyl rings excited to the imidotetrazine π^* orbitals. High-energy transitions in the region of 200 nm are solely due to phenyl ring π – π^* transitions.

Mechanism of Formation of Ylide 1. The formation of **1** instead of the expected product **3** or its valence tautomer **4** in a sequence of reactions from dichloride **2** is unexpected. This result is particularly surprising, considering that the observed product **1** is predicted to be thermodynamically less stable by 27 kcal/mol than the product of nucleophilic substitution at the imidoil carbon **3**, based on calculations for the parent species (vide infra).

The initial reaction of the dichloride **2** with sodium azide is well documented in the literature and yields mono-(**9-Z,Z**) and di-imidoil azides at ambient temperature.^{19–21} At higher tem-

(19) Stollé, R.; Netz, A. *Chem. Ber.* **1922**, 55, 1297–1305.

(20) Stollé, R.; Kramer, O.; Schick, E.; Erbe, H. *J. Prakt. Chem.* **1933**, 137, 327–338.

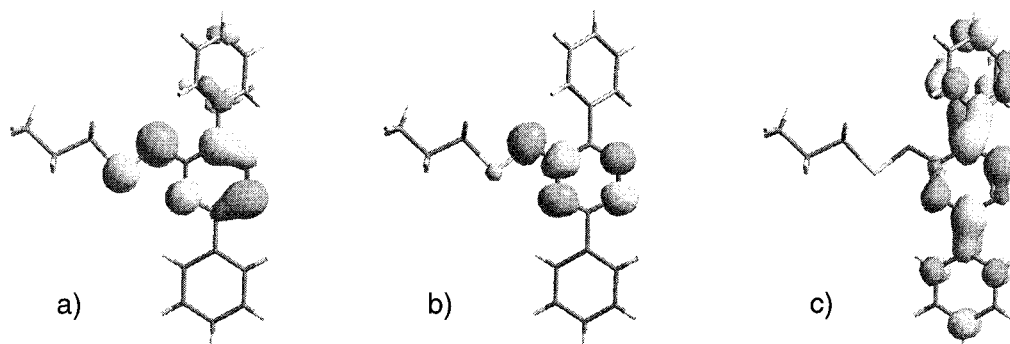
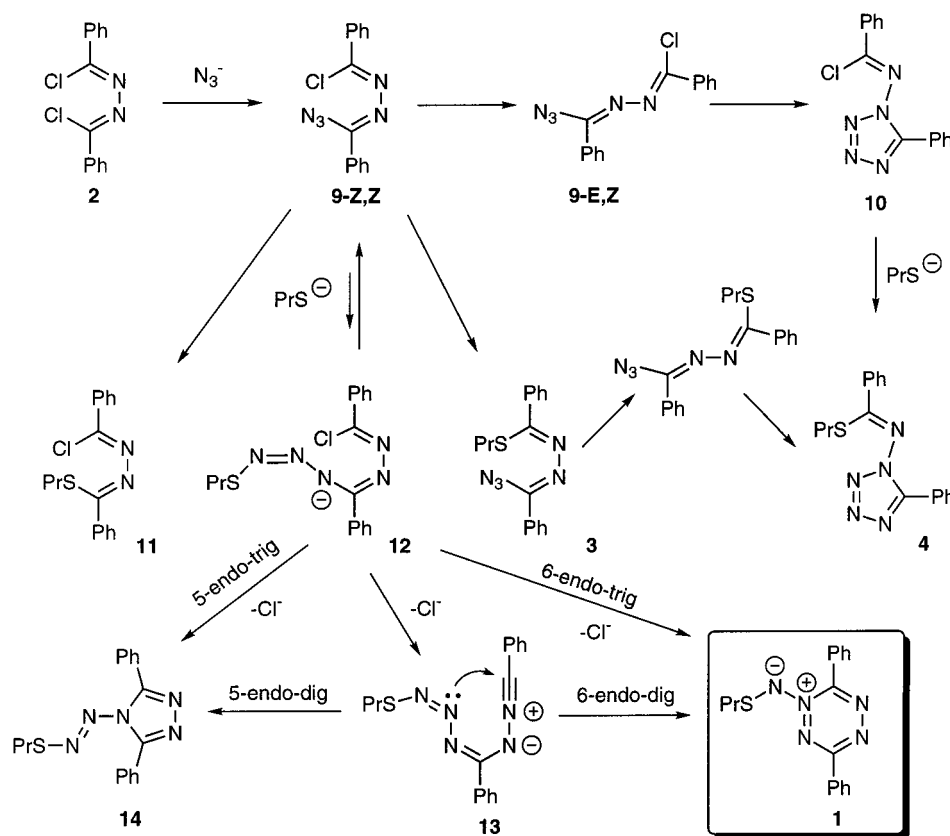


Figure 4. Representation of molecular orbitals calculated (ZINDO) for ylide **1** at the crystallographic coordinates: (a) the HOMO, (b) LUMO, and (c) the LUMO + 1.

Scheme 2



peratures, however, the imidoyl nitrogen atom undergoes isomerization to the E-isomer **9-E,Z**, which quickly cyclizes to tetrazole **10** (Scheme 2). The rate of the Z–E isomerization has been determined for similar compounds to be about 10^{-5} s^{-1} at 70°C with an activation energy of about 25 kcal/mol .⁴ Since the reaction of **2** with NaN_3 was conducted at ambient temperature, the formation of tetrazole **10** was slow and the mixture contained mostly the acyclic azide **9-Z,Z**.

The reaction of the azide **9-Z,Z** with a thiolate anion may proceed via three different pathways (Scheme 2): (i) nucleophilic displacement of the chloride and the formation of **3**, (ii) nucleophilic displacement of the azide and the formation of **11**, or (iii) nucleophilic addition to the azido group. The reaction, based on the molecular structure of **1**, must proceed according to path iii, and the thiolate anion must add to the terminal nitrogen atom of the N_3 group. The resulting intermediate **12** easily loses a chloride anion, forming nitrile imine **13** in accord with the general reactivity of hydrazoneyl chlorides with tertiary

amines.²² A subsequent intramolecular nucleophilic addition of the nitrogen lone pair to the electron-deficient nitrile carbon atom forms the six-membered ring of **1**. This mode of ring closure is favorable, according to Baldwin's rules,²³ and represents a rare example of a "6-endo-dig" ring closure.^{24,25} The NBO analysis and experimental molecular structure for **1** support this mechanism, showing a single C–N bond formed with the nitrogen electron lone pair (vide supra).

It is also conceivable, although less likely, that ylide **1** is formed directly from the adduct **12** by a "6-endo-trig" cycliza-

(22) Caramella, P.; Grünanger, P. In *1,3-Dipolar Cycloaddition Chemistry*; Padwa, A., Ed.; Wiley & Sons: New York, 1984; Vol. 1; pp 291–392 and references therein.

(23) Baldwin, J. E. *Chem. Commun.* **1976**, 734–736.

(24) Johnson, C. D. *Acc. Chem. Res.* **1993**, *26*, 476–482 and references therein.

(25) Jung, M. E. In *Comprehensive Organic Transformations*; Trost, B. M., Fleming, I., Eds.; Pergamon: New York 1991; Vol 4; pp 41–52; Regan, A. C. In *Comprehensive Organic Functional Group Transformations*; Katritzky, A. R., Meth-Cohn, O., Rees, C. W., Eds.; Pergamon: New York 1995; Vol. 1; pp 547–549 and references therein.

(21) Behringer, H.; Fischer, H. *J. Chem. Ber.* **1962**, *95*, 2546–2556.

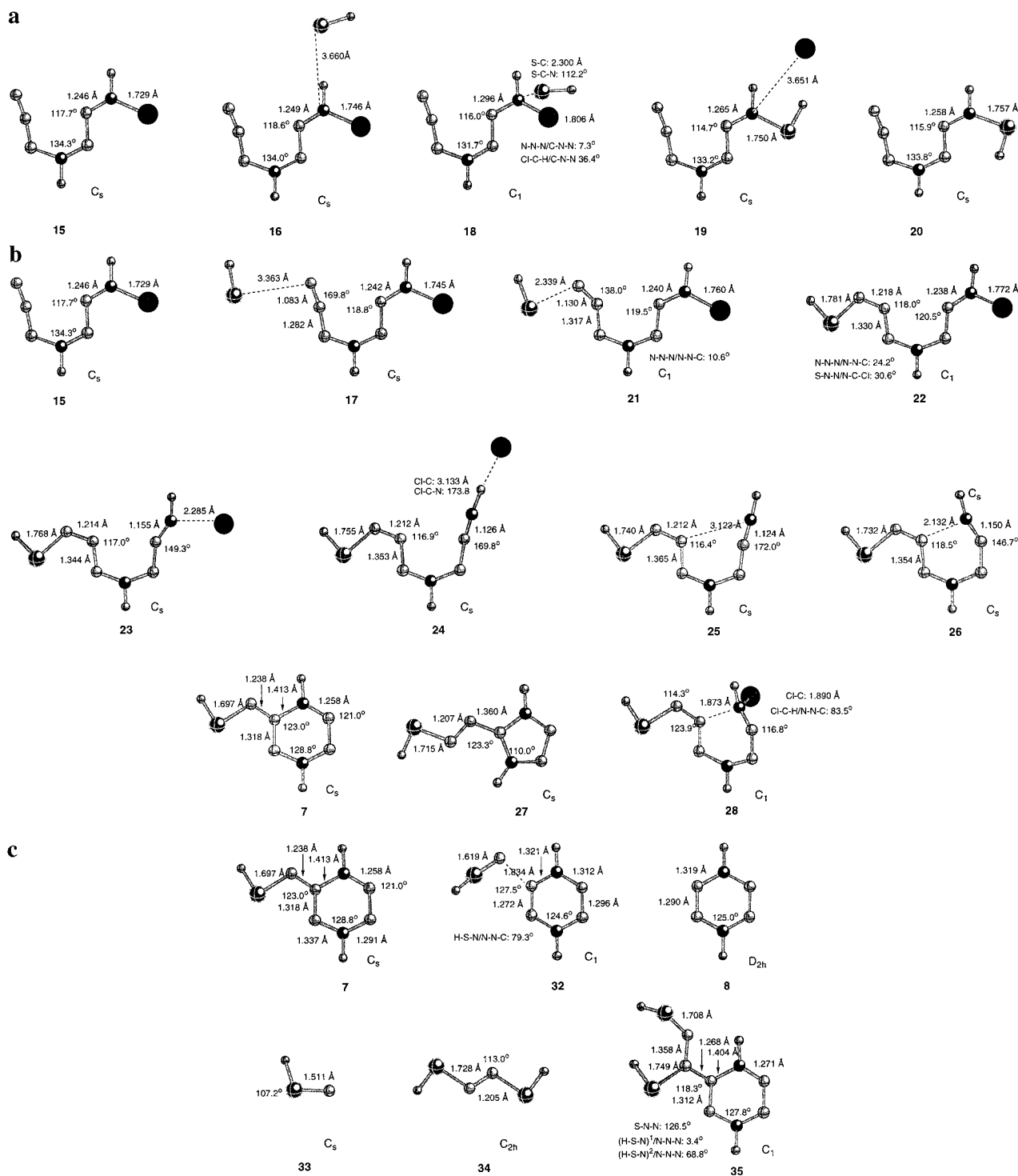


Figure 5. Optimized (HF/6-31+G*) geometries of the ground state and transition state structures, and pre- and post-transition complexes involved in (a) the nucleophilic substitution at the imidoyl carbon, (b) nucleophilic addition to the azido group, and (c) thermolysis of the ylide **7**.

tion and substitution of the imidoyl chloride. Alternatively, anion **12** or nitrile imine **13** could undergo a “5-endo” ring closure to form the five-membered ring of triazole **14**. The triazole is more thermodynamically stable than **1** by 31 kcal/mol, based on calculations for the parent species, but is not observed. The “5-endo-trig” reaction of **12** is disfavored,²³ and the formation of the triazole **14** from **13** requires an initial Z–E isomerization of the C=N bond, whose activation energy barrier is expected to be similar to that measured for **9**.

Since **1** is not the thermodynamic product, its formation must result from more favorable reaction kinetics. Support for this assertion is provided by the gas-phase reaction path calculation

for the formation of the expected (**3**) and the observed (**1**) products (Scheme 2). For simplicity, the substituents in ground-state and transition-state structures were replaced with hydrogen atoms (Figure 5). The results of ab initio calculations are collected in Table 2, and two potential energy curves for combined individual reactions are shown in Figure 6.

Imidoyl azide **15** and hydrogen sulfide are initially separated by infinite distance ($G_{298} = -1207.138401$ au, $\Delta G = 0$ kcal/mol). Deprotonation of the latter generates a hydrosulfide anion ($\Delta G = 347.4$ kcal/mol, experimental²⁶ 344.9 kcal/mol), which

(26) Gal, J.-F.; Maria, P.-C. In *Progress in Physical Organic Chemistry*; Taft, R. W., Ed.; Wiley & Sons: New York, 1990; Vol. 17; pp 159–238.

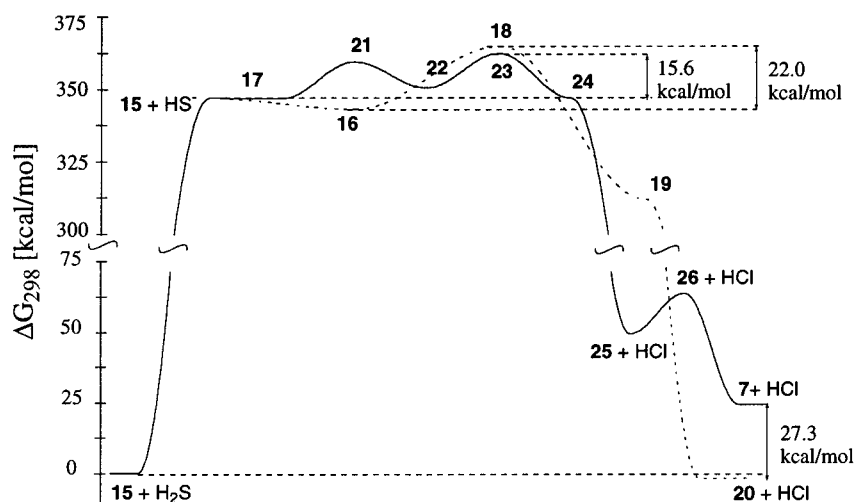


Figure 6. HF/6-31+G* Gibbs free-energy profiles (298 K) for the formation of tetrazine ylide **7** (solid line) and the imidoyl azide **20** (dashed line) in the gas phase. Transition- and ground-state structures are shown in Figure 5.

Table 2. Calculated (HF/6-31+G*) Relative Free Energies (kcal/mol) for Species Found on Potential Energy Surfaces in Figure 6 and Shown in Figure 5^a

compd	ΔG_{298} ($\Delta G_{298}^{\ddagger}$)
15 + H ₂ S	0
15 + HS ⁻	347.4
Formation of ylide 7	
17	347.3
21 (TS)	360.1 (+12.8)
22	351.0
23 (TS)	363.0 (+12.0)
24	347.4
25 + HCl	48.3
26 (TS) + HCl	62.4 (+14.1)
7 + HCl	23.6
Formation of azide 20	
16	343.6
18 (TS)	365.5 (+21.9)
19	312.4
20 + HCl	-3.7
Formation of triazole 27	
27 + HCl	-7.6

^a Full computational results are listed in the Supporting Information.

is allowed to interact with **15**. This leads to two shallow pre-transition minima in which the nucleophile assumes a coplanar orientation favorable for the addition to the imidoyl carbon (**16**) or to the azide (**17**). Both pre-transition structures are planar, and the energy of the former is lower than that of the latter by about 4 kcal/mol.

The subsequent nucleophilic substitution at the imidoyl carbon proceeds in one step through the tetrahedral transition state **18** (Figure 5a) and requires activation energy $\Delta G^{\ddagger} = 21.9$ kcal/mol. The resulting post-transition minimum, represented by **19**, is more stable than the pre-transition structure **16** by about 31 kcal/mol. Further stabilization is achieved by protonation of the Cl⁻ anion and separation of HCl from the product **20** to infinite distance. The overall transformation from **15** to **20** results in a net thermodynamic gain of about 4 kcal/mol.

The nucleophilic addition to the azido group and elimination of the chloride anion is a more complex, two-step process and is thermodynamically less favorable overall. The hydrosulfide anion adds to the terminal nitrogen atom and, through the transition state **21**, forms the intermediate anion **22** (Figure 5b). The reaction is endoergic by 3.7 kcal/mol and requires $\Delta G^{\ddagger} =$

12.8 kcal/mol of activation energy. The C–Cl bond in **22** is elongated by 2% relative to the azide **15**, which coincides with 0.1 *e* increase of the negative charge on chlorine.

The subsequent elimination of the chloride anion from **22** through the transition state **23** leads to the formation of the planar post-transition complex **24**. The overall two-step reaction from pre-transition complex **17** to **24** is thermoneutral and requires a total of $\Delta G^{\ddagger} = 15.7$ kcal/mol of activation energy. This is over 6 kcal/mol less than the activation energy for the nucleophilic displacement at the imidoyl carbon.

The protonation of the Cl⁻ anion in the post-transition complex **24** and removal to infinite distance as HCl (Et₃N·HCl in the reaction) yields nitrile imine **25**. The subsequent intramolecular cyclization of nitrile imine **25** through transition state **26** to form tetrazine **7** requires a small activation energy ΔG^{\ddagger} of about 14 kcal/mol and provides thermodynamic stabilization of 24.7 kcal/mol with respect to the nitrile imine **25**. Closure of the five-membered ring in nitrile imine **25** to form triazole **27** would provide an additional 31.2 kcal/mol of stabilization energy but is prevented by an energy barrier for the C=N double bond isomerization.

An alternative route to ylide **7** by direct cyclization of anion **22** includes a high-energy transition state represented by the nonplanar **28** ($\Delta G^{\ddagger} = 37.6$ kcal/mol). Therefore, the involvement of **28** in the formation of **1** is unlikely.

All intermediates and transition-state structures in the sequence from **15** to **7** are planar except for **21** and **22**, which exhibit small deviations from planarity. The progressive changes in the molecular geometries of the intermediates are shown in Figure 5.

The shape of the potential-energy surfaces in Figure 6 is a consequence of the gas-phase environment of the calculated reactions.^{27,28} Since both reaction pathways involve isomeric species, computational errors should be minimized, and a meaningful comparison of pairs of individual reactions can be made. For the same reason, the nonspecific solvation of the organic species by THF should be approximately similar, and hence the gas-phase thermodynamic calculations for the reactions should be at least a semi-quantitative representation of the relative energetics of solution processes. In contrast, an assessment of the overall thermodynamics for the transformation

(27) Riveros, J. M.; Jose, S. M.; Takashima, K. In *Advances in Physical Organic Chemistry*; Gold, V., Bethell, D., Eds.; Academic Press: New York, 1985; Vol. 21; pp 206–219.

(28) Shi, Z.; Boyd, R. J. *J. Am. Chem. Soc.* **1989**, *111*, 1575–1579.

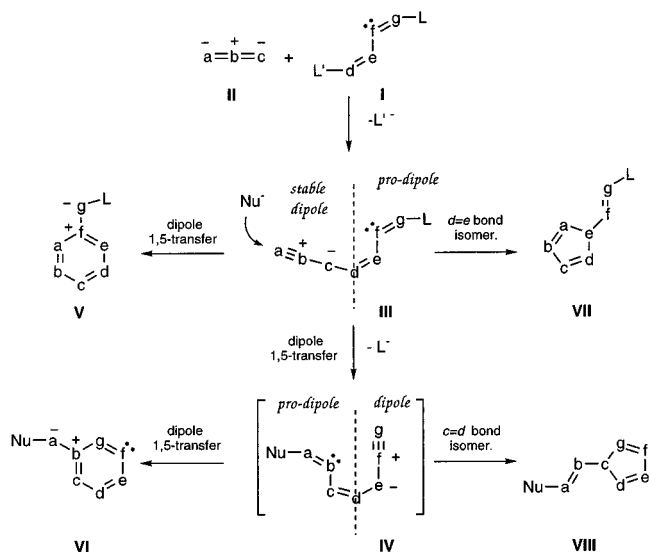


Figure 7. Generalized mechanism for the formation of **1**.

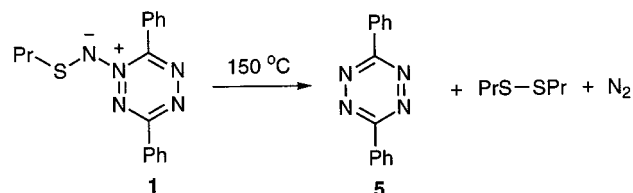
of **15** to **7** or to **20** is much more difficult to quantify than the individual reactions. The inorganic acids, HCl and H₂S, exhibit differential solvation and specific interactions with Et₃N which result from the difference in the gas-phase acidity (calcd 22.6 kcal/mol, experimental²⁶ 17.0 kcal/mol) among other factors. With correction for the difference in the acidity alone, the formation of ylide **7** from **15** is almost thermoneutral with respect to the starting materials, while the formation of **20** become exoergic by 26.3 kcal/mol.

Generalized Mechanism. The formation of the tetrazine ylide **1** can be presented as a sequence of general reactions shown in Figure 7. In the first step, a conjugated four-atom chain *defg* of **I** is extended to a seven-atom 1,7-dipole **III** via a nucleophilic substitution of the leaving group L' with a 1,3-dipole anion *abc* (–) (**II**). In the formation of **1**, the former represents dichloride **2**, and the latter is the N₃[–] anion. Addition of a nucleophile, Nu[–], to the 1,7-dipole **III** triggers the lone-pair-assisted departure of the second leaving group L and the net 1,5-transposition of the formal positive charge from *b* to *f* and formation of **IV**. Both conjugated dipoles, **III** and **IV**, may undergo “6-endo-dig” ring closure, accompanied by the net 1,5-transposition of the formal positive charge, and formation of cyclic conjugated dipoles **V** and **VI**, respectively. In these reactions the unshared electron pair of the n-orbital on *f* or *b* serves as a nucleophile, creating a new σ bond in **V** and **VI**, respectively. Alternatively, non-polar five-membered products **VII** (e.g., **10**) and **VIII** (e.g., **14**) can be formed after isomerization of the *d = e* or *c = d* bonds, respectively, followed by “5-endo-dig” ring closure.

The formation of the more thermodynamically stable non-polar five-membered rings (e.g., **27** in Figure 5b) is controlled by the height of the activation barrier for double bond isomerization, while the choice between the two six-membered rings, **V** and **VI**, depends on their relative thermodynamic stability. Thus, the successful formation of **VI** (e.g., **1**) requires (i) the presence of a lone pair on atom *f* (nitrogen atom in **2**), (ii) Z-configuration on the *d = e* and *c = d* double bonds in **III** and **IV** to prevent five-membered ring closure, (iii) stable intermediate **III**, (iv) significant activation barriers to Z–E isomerization in the 1,7-dipoles, and (v) lower thermodynamic stability of **V** with respect to **III** and **VI**.

These conditions are satisfied in the synthesis of **1** in which the addition of the thiolate to **III** is stereospecific.

Scheme 3



This scheme for preparation of **1** can, in principle, be extended to other structures, but the choice for the initial reagents appears rather limited. 1,4-Dichloro-2,3-diazabutadienes belong to a rare class of compounds suitable to serve as the L'-*defg*-L component **I** in Figure 7. There are two readily available stable 1,3-dipole anions, azide and diazomethyl²⁹ anions, that can be used as the *abc* anion **II** in the reaction. This combination of these reagents leads to tetrazine ylides, such as **1**, and may provide access to 1,2,4-triazine derivatives when CHN₂(–) is used.

A much wider variety of nucleophilic reagents Nu[–] could be expected to work in the sequence of the reactions in Figure 7. Besides thiolates, a number of C- and N-nucleophiles readily add to the azide or to the diazoalkyl groups, but the products are isolated only when the adduct can be kinetically or thermodynamically stabilized.^{30,31}

Reactivity of 1. Tetrazine ylide **1** can be viewed as a 1,7-dipole and also as a formal adduct of thionitrene to tetrazine **5**. Therefore, cleavage of the exocyclic N–N bond should be observed, and **1** should react with typical dipolarophiles.

Thermolysis. Despite the low decomposition temperature of the neat solid (102–103 °C), thermolysis of ylide **1** in boiling chlorobenzene was slow. In 1,2-dichlorobenzene, a higher boiling solvent, the decomposition proceeded at an appreciable rate. Tetrazine **5** and dipropyl disulfide were the dominant products and were easily identified by the characteristic red-pink color and the NMR spectra. Preparative scale thermolysis of **1** gave tetrazine **5** in 88% isolated yield (Scheme 3).

Thermolysis of **1** was monitored by ¹H NMR, showing very clean transformation of the ylide to tetrazine **5** (Figure 8). On the basis of the ratio of the resulting tetrazine **5** to starting ylide **1**, the decomposition of **1** in *o*-C₆D₄Cl₂ at 150 °C appears to be a first-order reaction with the rate $k = 1 \times 10^{-5} \text{ s}^{-1}$ (see Supporting Information).

The observation of tetrazine **5** and dipropyl disulfide in the reaction mixture suggests the intermediacy of propylsulfenyl nitrene **29**, which presumably dimerizes to form diazene **30** (Scheme 4). In this scenario, the initially formed tetrazine **5** and nitrene **29** are in equilibrium with ylide **1**, but the dimerization of the nitrene and the irreversible formation of diazene **30** shifts the reaction to the right. The diazene subsequently thermally decomposes under the reaction conditions to form the disulfide in about 50% yield, according to the NMR analysis. Alternatively, the nitrene **29** may attack the exocyclic nitrogen atom in ylide **1** to form the transient **31**, which subsequently would undergo elimination of tetrazine **5** and form diazene **30**. The latter mechanism would be consistent with general electrophilicity of the nitrene and the proposed path of disulfide formation during oxidative generation of sulfenyl nitrenes.³²

(29) Regitz, M.; Maas, G. *Diazo Compounds. Properties and Synthesis*; Academic Press: New York, 1986; pp 437–446.

(30) Sheradsky, T. In *The Chemistry of the Azido Group*; Patai, S., Ed.; Wiley & Sons: New York, 1971; pp 331–395.

(31) Engel, A. In *Organische Stickstoff-Verbindungen I*; Klamann, D., Ed.; Thieme: New York, 1990; Vol. E16a/II; pp 1182–1237.

(32) Atkinson, R. S.; Judkins, B. D. *J. Chem. Soc., Perkin Trans. 1* **1981**, 2615–2619.

Scheme 4

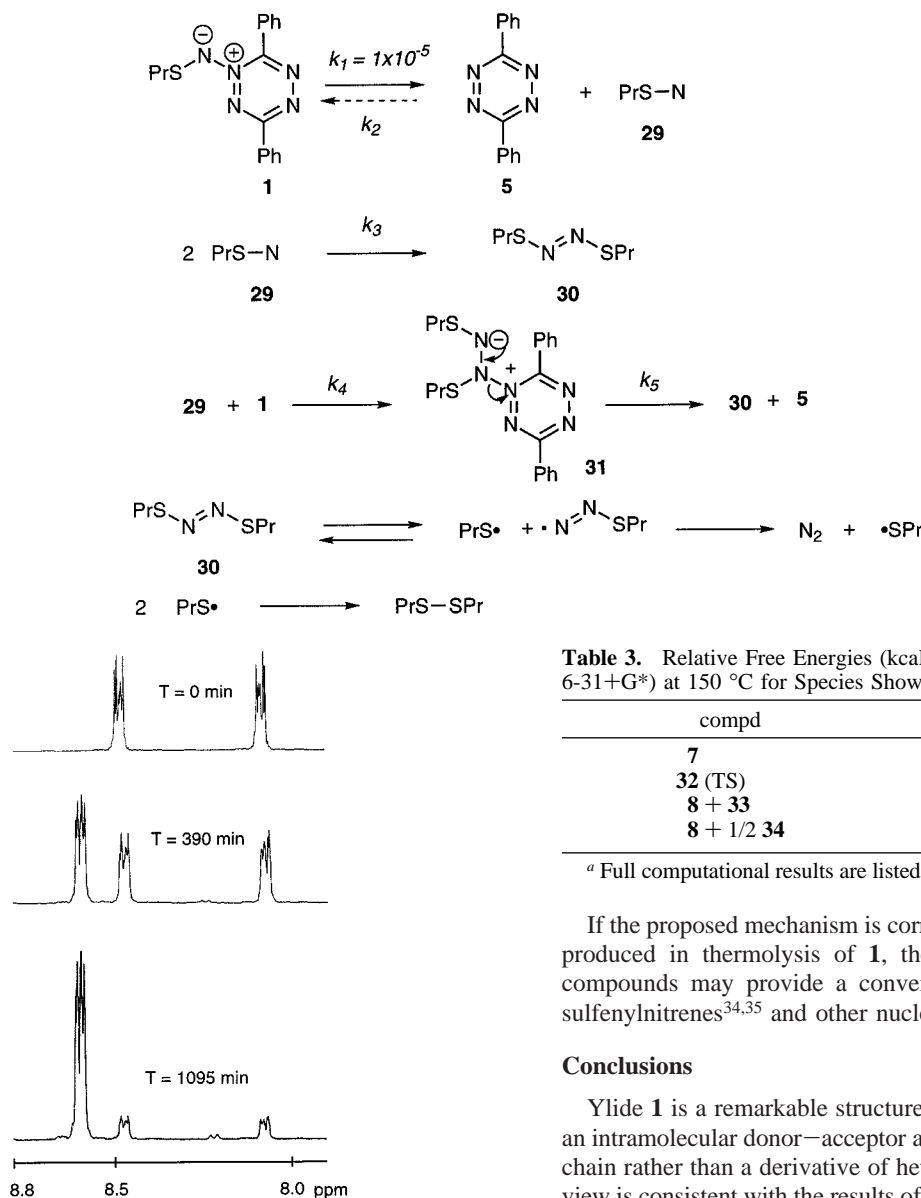


Figure 8. Low-field portion of NMR spectra of the thermolysis reaction mixture taken in $\text{C}_6\text{D}_4\text{Cl}_2$ at three time intervals. The top spectrum represents starting ylide **1**, and the increasing absorption at 8.34 ppm is due to the forming tetrazine **5**.

According to these mechanisms, the cleavage of the N–N bond and the formation of the nitrene is assumed to be the rate-determining step, and nitrene dimerization, either direct or through adduct **31**, is a much faster process ($k_1 \ll k_3, k_4, k_5$ in Scheme 4).

Ab initio calculations for the parent ylide **7** support the proposed mechanism. The heterolytic cleavage of the exocyclic N–N bond in ylide **7** proceeds via transition state **32** and requires $\Delta G^\ddagger = 33.1$ kcal/mol of activation energy (Figure 5c and Table 3). The formation of tetrazine **5** and the singlet $^1A'$ nitrene **33**³³ is endoergic by 4.4 kcal/mol, but the subsequent exoergic dimerization of the nitrene **33** to diazene **34** shifts the equilibrium to the right. The formation of the adduct **35** in the alternative mechanism for formation of diazene **34** is significantly endoergic by 27.0 kcal/mol and, perhaps, can be excluded.

(33) The $^1A'$ nitrene **33** used in this discussion is calculated to be more stable than the corresponding $^3A''$ triplet by 4.9 kcal/mol: Watts, J. D.; Huang, M.-J. *J. Phys. Chem.* **1995**, *99*, 5331–5335.

Table 3. Relative Free Energies (kcal/mol) Calculated (HF/6-31+G*) at 150 °C for Species Shown in Figure 5c^a

compd	ΔG_{423}
7	0
32 (TS)	33.1
8 + 33	4.4
8 + 1/2 34	–29.6

^a Full computational results are listed in the Supporting Information.

If the proposed mechanism is correct and nitrene **29** is indeed produced in thermolysis of **1**, then ylide **1** and analogous compounds may provide a convenient alternative source of sulfonylnitrenes^{34,35} and other nucleophilic nitrenes.³⁶

Conclusions

Ylide **1** is a remarkable structure which can be described as an intramolecular donor–acceptor adduct in a linear conjugated chain rather than a derivative of heteroaromatic tetrazine. This view is consistent with the results of X-ray analysis and ab initio calculations.

The formation of ylide **1** instead of the expected product **3** has been attributed to the more favorable kinetics in the former. Gas-phase ab initio calculations are consistent with the experimental results and show that the difference between the two reaction pathways is about 6 kcal/mol.

Furthermore, the formation of **1** is controlled by the cis geometry of the substrate and the stereoelectronics of the nucleophilic addition to the 1,7-dipole. The addition triggers the formation of a new conjugated 1,7-dipole, which cyclizes to form the six-membered ring in **1**. Generalization of this mechanism could extend this new reaction to other nucleophiles and to at least one other heterocyclic ring.

The thermolysis of **1** proceeds with first order kinetics and cleanly yields diphenyltetrazine **5**. One possible mechanism accounting for this reaction involves heterolytic cleavage of the exocyclic N–N bond in **1** and formation of a nitrene in the rate-determining step. This proposal is consistent with the results

(34) Atkinson, R. S.; Judkins, B. D.; Khan, N. *J. Chem. Soc., Perkin Trans. 1* **1982**, 2491–2497.

(35) Michida, T.; Sayo, H. *Chem. Pharm. Bull.* **1994**, *42*, 27–30.

(36) Deyrup, J. A. In *Small Ring Heterocycles*; Hassner, A., Ed.; Wiley & Sons: New York, 1983; Vol. 1; pp 62–69.

of ab initio calculations. Clearly, further studies and trapping experiments are necessary to support this mechanism and to account for the formation of the tetrazine.

Computational Methods

Ab initio calculations were carried out at the HF/6-31+G* level of theory using the Gaussian 94³⁷ package on SGI R8000 workstation, and the resulting energies are listed in Supporting Information. Appropriate symmetry constraints were used in geometry optimizations. Harmonic vibrational frequency analyses were performed for all stationary points. Zero-point vibrational energies (ZPE) and thermodynamic properties at 298 K were calculated using 0.9135 scaling factor.³⁸ Transition states were obtained using the TS keyword, and their connectivities to the appropriate minima were verified with the IRC calculation at the HF/3-21G*. ZINDO calculations were performed for **1** in the Cerius2 suite of programs using crystallographic atomic coordinates.

Experimental Section

NMR spectra were obtained on a Bruker instrument at 400 MHz (¹H spectra) and 75 MHz (¹³C) in CDCl₃ and referenced to TMS (¹H) or solvent (¹³C), unless specified otherwise. IR spectra were recorded using a Nicolet Magna 500 instrument in KBr unless specified otherwise. Mass spectrometry was performed using a Hewlett-Packard 5890 instrument (GCMS). Elemental analysis was provided by Atlantic Microlab, Norcross, GA. 1,2-Dichlorobenzene-*d*₄ was purchased from Aldrich, Milwaukee, WI, and used without further purification.

X-ray Crystallography for 3,6-Diphenyl-1-propanesulfenimido-1,2,4,5-tetrazine (1). A crystal of the compound was attached to a glass fiber and mounted on the Siemens SMART system for a data collection at 173(2) K. An initial set of cell constants was calculated from reflections harvested from three sets of 20 frames. These initial sets of frames are oriented such that orthogonal wedges of reciprocal space were surveyed. This produces orientation matrixes determined from 83 reflections. Final cell constants are calculated from a set of 4683 strong reflections from the actual data collection.

3,6-Diphenyl-1-propanesulfenimido-1,2,4,5-tetrazine (1). Dichloride **2** (277 mg, 1 mmol), NaN₃ (65 mg, 1 mmol) and benzyltriethylammonium chloride (15 mg) in dry THF (10 mL) were stirred at ambient temperature overnight under dry nitrogen. NMR spectrum of the crude mixture shows an apparent *td* at 8.08 ppm ($J_1 = 8.1$ Hz, $J_2 = 1.6$ Hz) in addition to signals belonging to the starting **2** in the ratio of 2:1. The presumed diazide (dd at 7.95 ppm, $J_1 = 8.5$ Hz, $J_2 = 1.5$ Hz) constitutes about 15% of the mixture.

1-Propanethiol (76 mg, 1 mmol) and Et₃N (101 mg, 1 mmol) were added to the resulting yellow suspension, and the mixture was stirred for 5 h under dry nitrogen. Solvents were removed under reduced pressure, and the orange solid residue was dissolved in a small amount

(37) Frisch, M. J.; Trucks, G. W.; Schlegel, H. B.; Gill, P. M.; Johnson, B. G.; Robb, M. A.; Cheeseman, J. R.; Keith, T.; Petersson, G. A.; Montgomery, J. A.; Raghavachari, K.; Al-Laham, M. A.; Zakrzewski, V. G.; Ortiz, J. V.; Foresman, J. B.; Cioslowski, J.; Stefanov, B. B.; Nanayakkara, A.; Challacombe, M.; Peng, C. Y.; Ayala, P. Y.; Chen, W.; Wong, M. W.; Andres, J. L.; Replogle, E. S.; Gomperts, R.; Martin, R. L.; Fox, D. J.; Binkley, J. S.; Defrees, D. J.; Baker, J.; Stewart, J. P.; Head-Gordon, M.; Gonzalez, C.; Pople, J. A. *Gaussian 94*, Revision E.1; Gaussian, Inc.: Pittsburgh, PA, 1995.

(38) Scott, A. P.; Radom, L. *J. Phys. Chem.* **1996**, *100*, 16502–16513.

of methylene chloride and deposited on a silica gel plug. The plug was eluted with a 2:1 hexanes–methylene chloride mixture to give 260 mg of a yellowish solid. Further washing of the plug with pure methylene chloride eluted an orange band which gave 260 mg of an oil containing largely the ylide **1**. Recrystallization of the oil from hexanes gave orange crystals: mp 102–103 °C dec; ¹H NMR (400 MHz) δ 1.09 (t, $J = 7.03$ Hz, 3H), 1.82–1.93 (m, 2H), 3.22 (t, $J = 7.2$ Hz, 2H), 7.35–7.59 (m, 6H), 8.06 (dd, $J_1 = 7.8$ Hz, $J_2 = 1.6$ Hz, 2H), 8.36 (dd, $J_1 = 7.7$ Hz, $J_2 = 1.7$ Hz, 2H); ¹³C NMR δ 13.14, 23.07, 38.93, 127.80, 128.10, 128.54, 128.86, 129.14, 131.19, 131.77, 132.40, 145.78, 160.53; IR 3065, 2963, 1603, 1531, 1473, 1405, 1365, 1213, 691 cm⁻¹; UV (cyclohexane), λ_{\max} (log ϵ) 368 (4.18) and 273 (4.42) nm. Anal. Calcd for C₁₇H₁₇N₅S: C, 63.13; H, 5.30; N, 21.65; S, 9.91. Found: C, 63.01; H, 5.29; N, 21.61; S, 9.84. Ylide **1** exhibits limited stability to silica gel. Substantial losses were noticed on fine 400–230 mesh gel and 100–60 mesh gel is recommended.

1,4-Dichloro-1,4-diphenyl-2,3-diaza-1,3-butadiene (2). It was obtained in 63% yield by chlorination of benzaldazine in CCl₄ at 50 °C, according to a literature procedure:³⁹ mp 117–119 °C (lit.³⁹ 121–122 °C); ¹H NMR δ 7.45–7.54 (m, 6H), 8.12–8.15 (m, 4H); ¹³C NMR δ 128.54 (2C), 131.80, 133.62, 144.20; EIMS, *m/z*, 280 (6), 278 (34), 276 (54), 243 (18), 241 (54), 138 (100), 103 (45), 77 (86).

Thermal Decomposition of Ylide 1. Kinetic Measurements. Tetrazine ylide **1** (7 mg) was dissolved in dry 1,2-dichlorobenzene-*d*₄ [¹H NMR δ 0.95 (t, 7.3 Hz, 3H), 1.72–1.80 (m, 2H), 3.03 (t, $J = 7.2$ Hz, 2H), 7.35–7.38 (m, 3H), 7.41–7.44 (m, 3H), 8.06–8.08 (m, 2H), 8.47–8.49 (m, 2H)] and heated in a sealed NMR tube at 150 ± 1 °C under dry nitrogen. The sample was occasionally cooled to ambient temperature, and the ratio of the product, 3,6-diphenyl-1,2,4,5-tetrazine [**5**; ¹H NMR δ 7.44–7.47 (m, 3H), 8.59–8.62 (m, 2H)] to the starting ylide **1** was monitored by ¹H NMR (400 MHz). Dipropyl disulfide [¹H NMR δ 0.89 (t, $J = 7.3$ Hz, 3H), 1.59–1.66 (m, 2H), 2.54 (t, $J = 7.2$ Hz, 2H)] was identified as the major byproduct. The identification of **5** and the disulfide in the mixture was confirmed by NMR of the pure compounds in the same solvent.

3,6-Diphenyl-1,2,4,5-tetrazine (5). Ylide **1** (94 mg, mmol) was dissolved in dry 1,2-dichlorobenzene and heated at 150 °C for 2.5 days under dry nitrogen. Volatiles were removed under reduced pressure, and the dark red residue was purified on a Chromatotron (CH₂Cl₂–hexanes, 1:1) giving 60 mg (88% yield) of **5** as red-purple needles: mp 195.5 °C (lit.⁴⁰ mp 197–198 °C); ¹H NMR δ 7.62–7.66 (m, 6H), 8.65–8.69 (m, 4H) [lit.⁴⁰ δ 7.77 (m, 6H), 8.8 (dd, 4H)].

Acknowledgment. This project has been supported by NSF (CHE-9528029).

Supporting Information Available: Tables of crystal data, structure solution and refinement, atomic coordinates, bond lengths and angles, and anisotropic thermal parameters along with a decomposition kinetic plot for **1**, representation of FMOs of **7**, and a list of computed energies for structures discussed in the text (PDF) and an X-ray crystallographic file in CIF format. This material is available free of charge via the Internet at <http://pubs.acs.org>.

JA993884Z

(39) Flowers, W. T.; Taylor, D. R.; Tipping, A. E.; Wright, C. N. *J. Chem. Soc. (C)* **1971**, 1986–1991.

(40) Barrett, A. G. M.; Read, R. W.; Barton, D. H. R. *J. Chem. Soc., Perkin Trans. 1* **1980**, 2184–2190.